Chapter 2
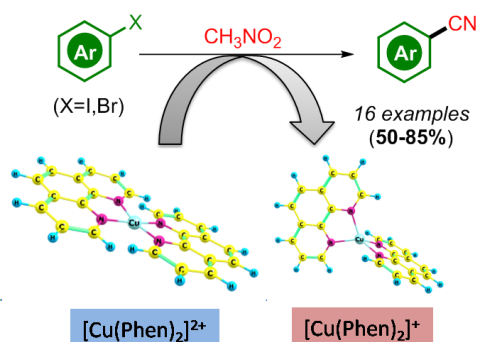
Cyanation

An Insight into Nitromethane as an Organic Nitrile Alternative Source towards the Synthesis of Aryl Nitriles

Rakhee Saikia,[a] Satyajit Dey Baruah,[a] Ramesh C. Deka,[a] Ashim J. Thakur,*[b] and Utpal Bora*[b]

$Ar-X$ CH_3NO_2 $Ar-CN$

(X=I,Br)

16 examples
(50-85%)

$[Cu(Phen)_2]^{2+}$ $[Cu(Phen)_2]^+$

- *In situ* reduction of Cu^{2+} to Cu$^+$
- Easily available starting material
- Non-toxic, cheap, organic cyanating source
- Operational Simplicity
- Wide substrate scope
- Computational study of evolution of CN$^-$

ABSTRACT: Directed by an unusual *in situ* reduction of Cu^{II}, this chapter discusses a simple Cu^I-mediated synthesis of aryl nitriles, with inexpensive and readily available nitromethane as the cyanating source. Exhibiting a wide substrate scope, the method involves simple reaction conditions, is additive–free with low catalyst loading. The mechanism of cyanation of aryl halides is elucidated by a congregation of three cycles, i.e. the *in situ* reduction of Cu^{II} species by nitromethane, generation of HCN species from nitromethane and a regular organometallic pathway which releases the nitrile derivative. The detail of the mechanism of generation of CN$^-$ from nitromethane is computationally validated. Our protocol holds the distinction of involving a rarely encountered Cu^I catalytic species as well as facile *in situ* generation of nucleophilic CN$^-$ to yield synthetically useful aromatic nitriles in moderate to good yields.

Chapter 2

2. Nitromethane: an alternative organic nitrile source!

2.1 *Introduction*

The exploration of novel methodologies for the introduction of a nitrile group into an aromatic framework is a much desired endeavour, as discussed in chapter 1 [1]. Since the first nitrile synthesis with Rosenmund−von Braun and Sandmeyer reactions being the breakthrough protocols, all the traditional methods of nitrile synthesis suffered from the use of stoichiometric amounts of toxic metal cyanides (M−CN; M= alkali metal, Cu, Zn, Ag etc.) and requirement of elevated temperatures (150-250 °C) among other drawbacks of the processes. One of the practical solutions that have emerged to reduce the risk of hazardous metal cyanides was to employ "indirect" cyanide sources. The indirect cyanide sources do not contain a directly linked −CN unit to the molecular skeleton, but they can produce CN⁻ *in situ* under suitable reaction conditions. Some of the reported indirect cyanide sources are *t*-BuNC [2-4], DMF [5-8], formamide [9-14] and nitromethane (Figure **2.1**).
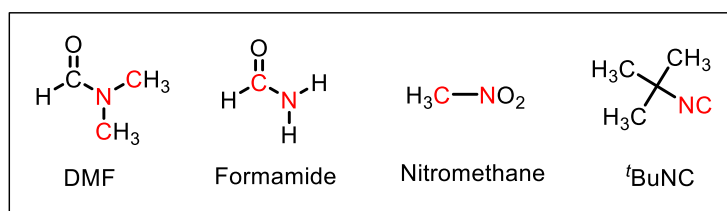

Figure **2.1** Examples of indirect cyanating sources

Although, a variety of transition metals, such as Fe [15], Pd [16], Ni [17], Co [18], Zn [19], Rh [20] and Ru [21] have been identified to assist the process of cyanation without the need of pre−functionalised substrates [22], the role of Cu as an inexpensive and readily available transition metal cannot be overlooked in cyanation [23]. Moreover, efficient and sustainable processes of cyanation of common functionalized substrates like aryl halides, needs further exploration [24].

A reagent and a useful reaction medium, nitromethane is an efficient cyanating source on account of its easy accessibility, inexpensiveness and non-toxicity. This chapter

discusses how nitromethane can be utilized as a mild and safe cyanating source for the synthesis of pharmaceutically significant aryl nitriles.
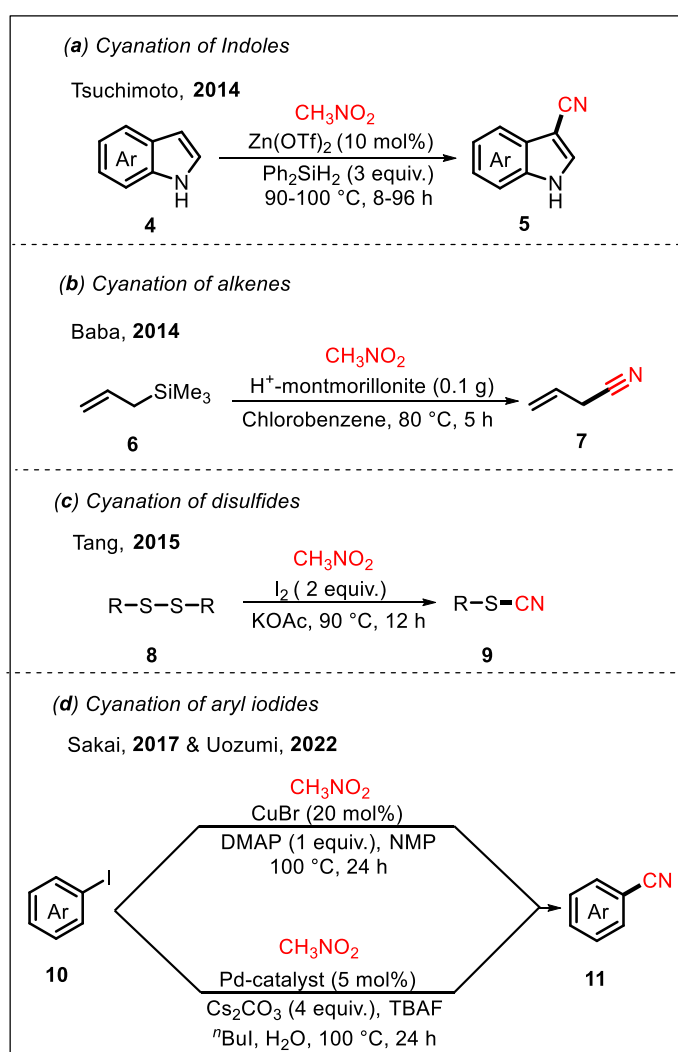
2.2 Background

The pioneers of employing the inexpensive, less-toxic and readily available indirect organic nitrile source CH_3NO_2, Yu and his group, successfully cyanated 2-Phenylpyridine (**1**) with nitromethane (Scheme **2.1**). The mechanism of the reaction was rationalized to occur *via* a radical-cation pathway, where the radical–cation was expected to form by transfer of a single electron (SET) from the aryl ring to the coordinated Cu (**A**). This was assumed to be the rate-determining step [25].
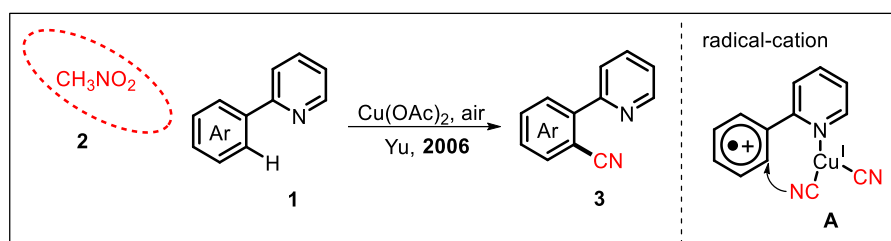
Scheme **2.1** First work on cyanation with nitromethane

Later in 2014, the research groups of Tsuchimoto and Baba independently developed two methodologies of cyanation with nitromethane. They utilized nitromethane to avoid toxic cyanide sources and generate synthetically useful aryl nitriles. Nitromethane could cyanate organic scaffolds with operational simplicity and economic viability. The former group utilized a combination of a Lewis acid, $Zn(OTf)_2$ and Ph_2SiH_2 for direct cyanation of C-H bonds of indoles/pyrroles (**5**) with nitromethane (Scheme **2.2a**) [19]. The methodology was further applied in the synthesis of a biologically relevant indolo[3,2-*c*]quinoline scaffold. In the latter attempt, Baba and his research group achieved cyanation of allyltrimethylsilanes (**6**) with proton-exchanged montmorillonite as the Brønsted acid and nitromethane as the cyanation source [26]. The nitrile–oxide generated by the reaction between nitromethane and (**6**) underwent 1,3-dipolar cycloaddition with another molecule of allyltrimethylsilane followed by subsequent rearrangement to yield the cyanated product (**7**) (Scheme **2.2b**). However, both the protocols employed a large excess of nitromethane. In another interesting approach, Wang et al. utilized nitromethane to develop a simple and effective I_2 mediated

synthesis of thiocyanates (**9**) (Scheme **2.2c**) [27]. The combination of I_2 and base was found necessary for the cleavage of S−S bond. The protocol was an important contribution for the metal−free synthesis of thiocyanates. It however, employed about "5 equivalents" of the base. On similar lines, Sakai and his group cyanated readily available aryl iodides (**10**) with nitromethane and CuBr as the catalyst (Scheme **2.2d**) [28]. The combination of DMAP and *N*-methylpiperidine (NMP) helped to obtain moderate to good yields of benzonitriles (**11**). On the other hand, Suzuka et al. designed an amphiphilic polymer-supported Pd−catalyst for the cyanation of aryl iodides (**10**) with nitromethane in water (Scheme **2.2d**) [29].

(a) Cyanation of Indoles

Tsuchimoto, **2014**

CH_3NO_2
Zn(OTf)$_2$ (10 mol%)
Ph$_2$SiH$_2$ (3 equiv.)
90-100 °C, 8-96 h

4 → **5**

(b) Cyanation of alkenes

Baba, **2014**

CH_3NO_2
H$^+$-montmorillonite (0.1 g)
Chlorobenzene, 80 °C, 5 h

6 → **7**

(c) Cyanation of disulfides

Tang, **2015**

CH_3NO_2
I$_2$ (2 equiv.)
KOAc, 90 °C, 12 h

R−S−S−R → R−S−CN

8 → **9**

(d) Cyanation of aryl iodides

Sakai, **2017** & Uozumi, **2022**

CH_3NO_2
CuBr (20 mol%)
DMAP (1 equiv.), NMP
100 °C, 24 h

CH_3NO_2
Pd-catalyst (5 mol%)
Cs$_2$CO$_3$ (4 equiv.), TBAF
^{n}BuI, H$_2$O, 100 °C, 24 h

10 → **11**

Scheme **2.2** Previous works on cyanation with nitromethane

Although an interesting development of cyanation with nitromethane, both the methodologies used super−stoichiometric amounts of nitromethane and large

equivalents of base. The methods also displayed a limited substrate scope of aryl iodides.

2.3 *Results and Discussion*

In this chapter, Cu^I–catalyzed cyanation of aryl halides (iodides and bromides) with nitromethane is discussed. The abundance of aryl halides in nature and their affinity towards a metal in a metal-catalyzed reaction makes them attractive substrates for cyanation. The developed protocol highlights an unprecedented, dual role played by nitromethane in the reaction. In addition to being the cyanating source, nitromethane also helped in the *in situ* generation of active Cu^I species by reduction of the parent Cu^{II} salt. The mechanistic aspect of our protocol is discussed in detail and supported by computational calculations. Moreover, it involves mild reaction conditions, low catalyst loading and requires no additives. To the best of our knowledge, mechanistic aspects of Cu-catalyzed cyanation of aryl iodides with nitromethane have not been explored in detail.

At first, a mixture of 4−Iodoanisole (**12a**), nitromethane (**2**) and a catalytic amount of CuCl$_2$ were made to react with each other in DMF. Although aromatic nitromethylation was the expected product, after 16 hours under reflux condition, the reaction offered an unexpected cyanated product in 71% yield. When the reaction was allowed to proceed beyond 16 hours, there was no increase in the yield of the cyanated product.

2.3.1 *Optimization of reaction conditions*

With 4-Iodoanisole (**12a**) as the model substrate, we optimized various reaction conditions that were suitable for cyanation and the obtained results are shown in Table **2.1**. With the reaction temperature maintained at 100 °C, it was found that when the reaction was carried out in nitromethane; both as the cyanating source and as a solvent, no cyanated product was obtained (Table **2.1**, entry **1**). As we shifted to other available protic and aprotic solvents like CH$_3$OH, CH$_3$CN, DMF and DMSO, best results were obtained in DMSO (Table **2.1**, entries **1**-**6**). With DMSO as the solvent, organic bases like (C$_2$H$_5$)$_3$N and DABCO and inorganic bases like K$_2$CO$_3$, NaOH and NaHCO$_3$ were also tested for cyanation (Table **2.1**, entries **7**-**10**). K$_2$CO$_3$ was found to exhibit the best activity under the given reaction conditions. Although both Cu(I) and Cu(II) salts could

easily facilitate cyanation (Table **2.1**, entries **11**-**14**), the reaction proceeded best with 5 mol% of $Cu(NO_3)_2 \cdot 3H_2O$.

Table 2.1 Initial investigation of reaction conditions for the Cu^I–catalyzed cyanation of 4−Iodoanisole (**12a**) with nitromethane (**2**).[a]
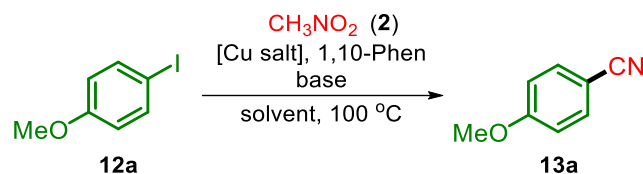
Entry	Base	Cu-salt	Solvent	Yield[b] (%)
1	K_2CO_3	$Cu(NO_3)_2 \cdot 3H_2O$	CH_3NO_2	-
2	K_2CO_3	$Cu(NO_3)_2 \cdot 3H_2O$	CH_3OH	67
3	K_2CO_3	$Cu(NO_3)_2 \cdot 3H_2O$	CH_3CN	73
4	K_2CO_3	$Cu(NO_3)_2 \cdot 3H_2O$	DMF	83
5	**K_2CO_3**	**$Cu(NO_3)_2 \cdot 3H_2O$**	**DMSO**	**85**
6	K_2CO_3	$Cu(NO_3)_2 \cdot 3H_2O$	Toluene	62
7	NaOH	$Cu(NO_3)_2 \cdot 3H_2O$	DMSO	70
8	$(C_2H_5)_3N$	$Cu(NO_3)_2 \cdot 3H_2O$	DMSO	57
9	DABCO	$Cu(NO_3)_2 \cdot 3H_2O$	DMSO	59
10	$NaHCO_3$	$Cu(NO_3)_2 \cdot 3H_2O$	DMSO	61
11	K_2CO_3	$Cu(OAc)_2 \cdot H_2O$	DMSO	62
12	K_2CO_3	$CuCl_2$	DMSO	83
13	K_2CO_3	CuCl	DMSO	67
14	K_2CO_3	CuI	DMSO	64
15[c]	K_2CO_3	$Cu(NO_3)_2 \cdot 3H_2O$	DMSO	65
16[d]	K_2CO_3	$Cu(NO_3)_2 \cdot 3H_2O$	DMSO	77
17[e]	K_2CO_3	$Cu(NO_3)_2 \cdot 3H_2O$	DMSO	62
18[f]	K_2CO_3	$Cu(NO_3)_2 \cdot 3H_2O$	DMSO	85

[a]*Reaction conditions:* 4−Iodoanisole, **12a** (1 mmol), nitromethane, **2** (1.5 equiv.), Cu−salt (5 mol%), ligand (10 mol%), base (1 equiv.), solvent (3 mL), 100 °C, 16 h; 1,10-Phen = 1,10-Phenanthroline monohydrate; [b]Isolated yield based on 4−Iodoanisole **12a**; [c]*N,N'*-dimethylurea was used as a ligand; [d]2,2'-Bipyridyl was used as a ligand; [e],[f]Reaction temperature was maintained at 80 °C and 120 °C respectively.

Its complexation with 10 mol% of 1,10−Phen *in situ*, among other ligands like *N,N'*−dimethylurea and 2,2'−Bipyridyl provided a better yield in shorter reaction time

(Table **2.1**, entries **15** and **16**). A decrease in temperature from 100 °C resulted in a significant decrease in product yield (Table **2.1**, entry **17**), while further increase in temperature to 120 °C (Table **2.1**, entry **18**) gave identical yield of the desired product as that obtained in entry **5**. Hence, the optimized reaction condition was fixed at 5 mol% of Cu(NO$_3$)$_2$·3H$_2$O and 10 mol% of 1,10−Phen with K$_2$CO$_3$ as the base in DMSO solvent.

2.3.2 *Substrate Scope Study*

Post optimization, the results of scope exploration of the Cu^I−catalyzed cyanation of aryl iodides and bromides are presented in Table **2.2**.

Table 2.2 Scope exploration of the Cu^I−catalyzed cyanation of aryl iodides and bromides (**12**) with nitromethane (**2**) as the cyanating source.[a]
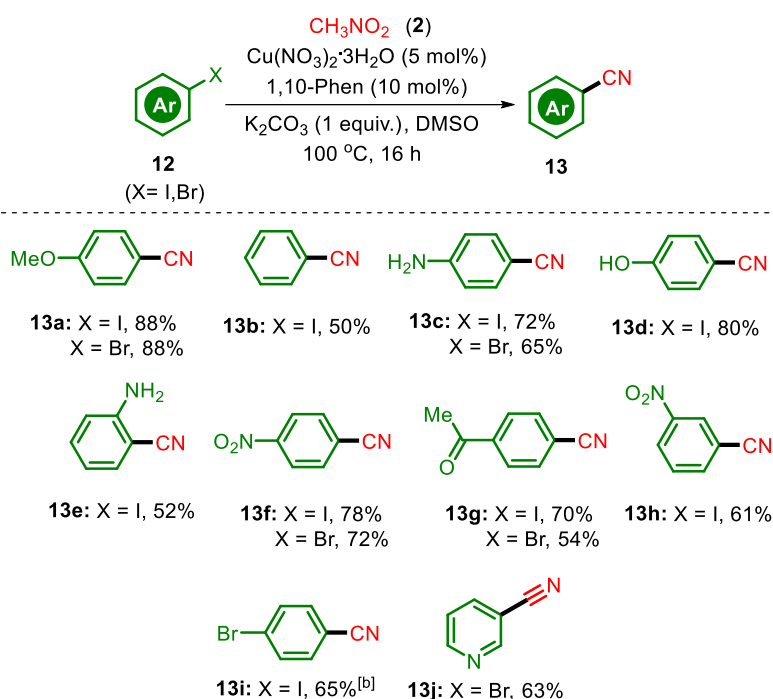
[a]*Reaction conditions:* Aryl halide, **12** (1 mmol), nitromethane, **2** (1.5 equiv.), Cu(NO$_3$)$_2$·3H$_2$O (5 mol%), 1,10−Phen (10 mol%), K$_2$CO$_3$ (1 equiv.), DMSO (3 mL), 100 °C, 16 h (the reaction time was not optimized for each substrate), [b]4−Iodobenzonitrile was obtained as the minor product (GC yield = 31%).

Various *o*-, *m*- and *p*-substituted aryl iodides and bromides have reacted with nitromethane under the optimized reaction condition (Table **2.1**, entry **5**) to give the corresponding cyanated product in moderate to good yields (Table **2.2**, entries **13a**-**k**). A decent range of electron withdrawing and electron donating groups have reacted to

afford the desired product in 52-85% yields. Nitromethane (**2**) cyanated all the substituted aryl iodides and bromides selectively at the aryl C–X (X= I/Br) bond. Electron releasing groups have shown a higher reaction yield in comparison to electron withdrawing groups. This could be attributed to the positive inductive effect of the electron-releasing substituents. The optimized reaction conditions tended to favour *p*-substituted aryl halides more than the *o*- and *m*- substitutes. Additionally, we obtained two interesting results during the study of substrate scope under the developed optimized reaction condition (Scheme **2.3**). 1–Iodo–2–nitrobenzene underwent cyanation with simultaneous reduction of the nitro group in 73% yield (Scheme **2.3**, **13e**). To investigate this, nitrobenzene was made to react under the same reaction conditions and aniline was obtained. This may be due to the reducing tendency of DMSO [30]. However, no such transformation was observed for the *m*- and *p*-analogues (Table **2.2**, **13f** and **13h**). On the other hand, benzyl bromide underwent nucleophilic substitution reaction to yield benzyl cyanide under the same reaction condition (Scheme **2.3**, **13k**). This observation hints at the release of HCN in the reaction medium.
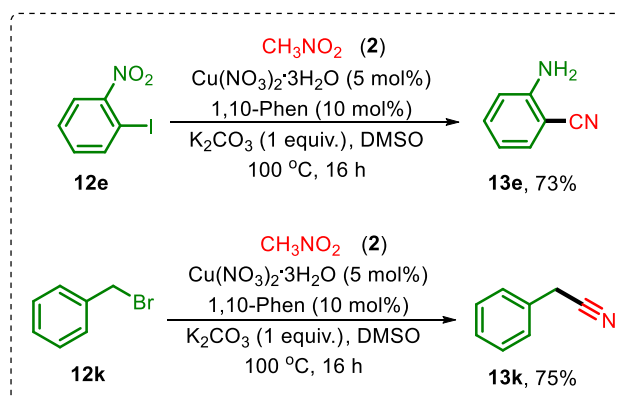
Scheme **2.3** Anomalous observations under the optimized reaction condition

2.3.3. *Mechanistic Study*

The mechanistic study of the reaction began with the isolation of a $[Cu(phen)_2]^{2+}$ complex (For details, see Section 2.3.7.4). The obtained $[Cu(phen)_2]^{2+}$ complex was then reacted with 4-Iodoanisole (**12a**) and nitromethane (**2**) to give the cyanated product (**13a**). Interestingly, we found that the active catalyzing species of the reaction was its

cuprous analogue formed through an unusual *in situ* reduction of $[Cu(phen)_2]^{2+}$ in the presence of nitromethane.

The formation of Cu^I in the reaction medium was confirmed by UV-Vis spectroscopy, cyclic voltammetry and EPR spectroscopy (Figure **2.2**). The broad absorption band at 420 nm is a characteristic of the MLCT electronic transition in $[Cu(phen)_2]^+$ complex corresponding to the transfer of an electron from a 3d orbital of Cu to antibonding π^* orbital of 1,10–Phen ligand (Figure **2.2a**) [31]. In 0.1 M KCl, the reaction mixture showed an anodic peak potential at 0.936 V vs Ag/AgCl which suggested oxidation of Cu^I to Cu^{II} and a cathodic peak potential at −0.173 V vs Ag/AgCl suggesting reduction of Cu^{II} to Cu^I, at a scan rate of 50 mV/s (Figure **2.2b**) [32]. X–band EPR spectra before the start of reaction, showed a sharp band with $g_∥$ = 2.26 and $g_⊥$ = 2.17 which was characteristic of Cu^{II} ion (Figure **2.2c**) [33]. The decrease in intensity of the EPR signal recorded for the reaction mixture after 16 hours confirmed the irreversible reduction of Cu^{II} to Cu^I during the reaction. Cu^I being a d^{10} ion, is diamagnetic. The UV-Vis, CV and EPR data confirmed the change in oxidation state of Cu from +2 to +1 during the reaction.
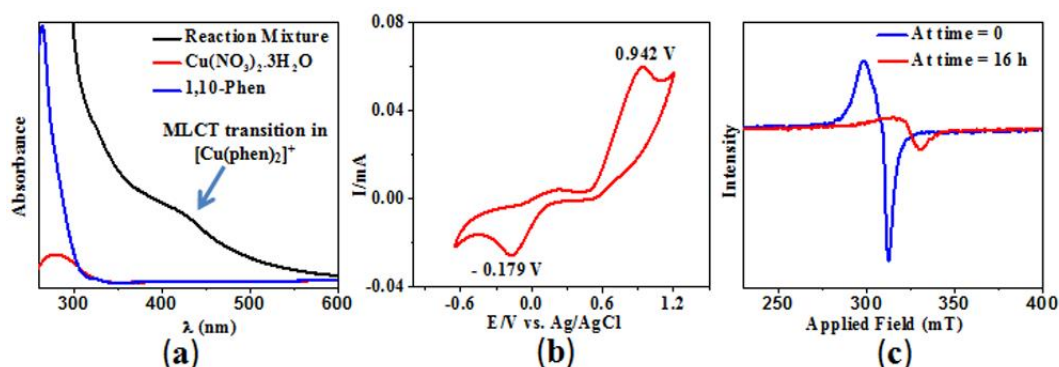

Figure **2.2** (**a**) UV-Vis spectra of [black: *in situ* generated Cu^I–complex; blue: 1,10-Phen; red: $Cu(NO_3)_2 \cdot 3H_2O$] in DMSO; (**b**) Cyclic Voltammogram of the reaction mixture recorded in *n*-Bu$_4$NClO$_4$/DMSO; (**c**) X–band EPR spectra of [blue: reaction mixture before the start of reaction; red: reaction mixture at the end of reaction i.e. 16 hours] in DMSO at 100 K.

The reduction of Cu^{II} to Cu^I took place only in the presence of nitromethane. Controlled experiment also supported the involvement of Cu in the facile release of CN⁻ (Scheme **2.4**). Since the formation of benzyl cyanide from benzyl bromide does not involve the usual organometallic cycle, failure to yield the cyanated product in absence of Cu,

suggested that Cu played an important role in the evolution of CN⁻ from nitromethane. The *in situ* generation of CN⁻ was further supported by the picrate paper test [34].
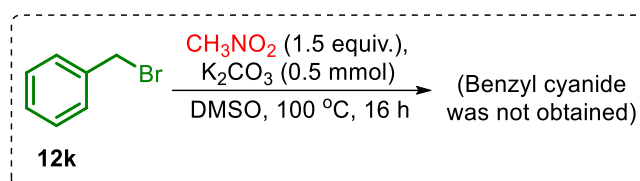
Scheme **2.4** No cyanation of benzyl bromide in the absence of Cu.

2.3.4 *Plausible Mechanism*

The reaction mechanism can be divided into three stages, viz., (**A**) the reduction of $[Cu(phen)_2]^{2+}$ to $[Cu(phen)_2]^+$ by nitromethane; (**B**) generation of HCN from nitromethane and (**C**) the general organometallic cycle involving oxidative addition, ligand exchange and reductive elimination to yield the desired nitrile derivative (Figure **2.3**).
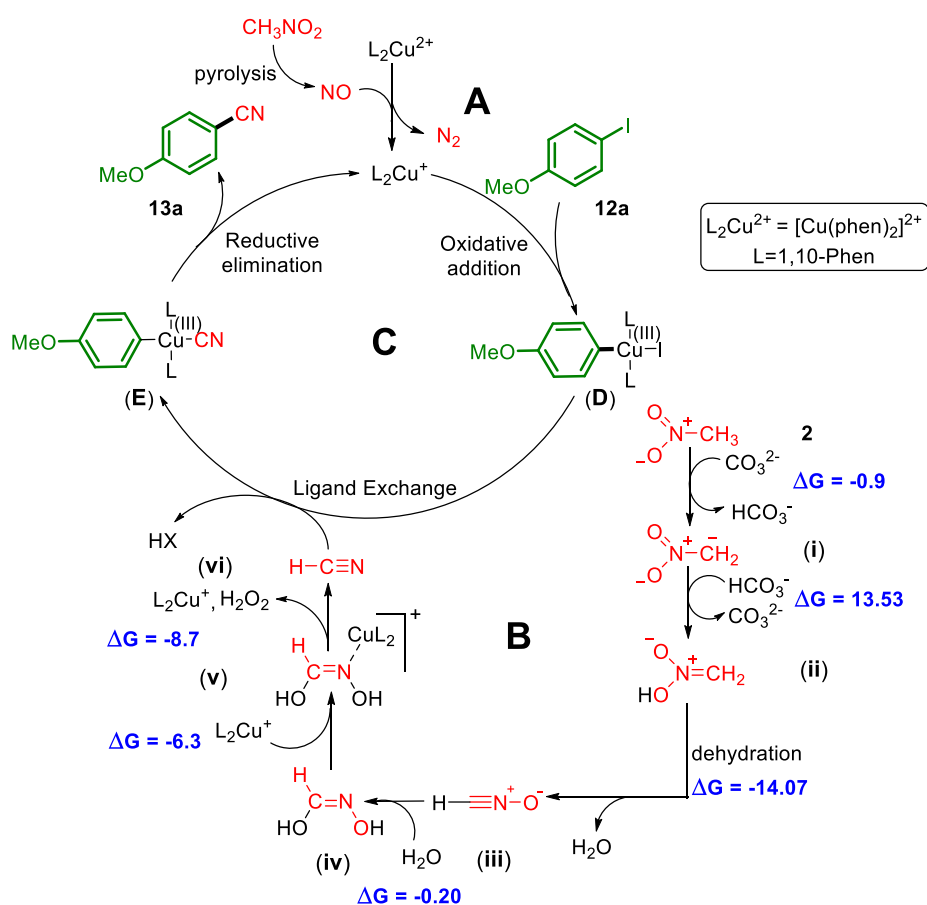

Figure **2.3** Plausible mechanism of cyanation

Studies on the thermochemistry of nitromethane showed that its decomposition at high temperatures can be subdivided into many phases with different products in each stage. Two of such important decomposition products are CO and NO [35] i.e. oxidation of the carbon atom of CH_3NO_2 to CO with subsequent reduction of the nitrogen atom to N_2 *via* the formation of NO [36]. The released NO interacts with Cu(II) in the reaction medium, causing the reduction of $[Cu(phen)_2]^{2+}$ to $[Cu(phen)_2]^+$ (Figure **2.3**, **A**) [37].

From previous literature, the process of generation of HCN from nitromethane (Figure **2.3**, **B**) can be rationalized through proton abstraction (**i**) (the reaction does not proceed in the absence of a base), followed by dehydration of (**ii**) to form the nitrile oxide (**iii**). The generated nitrile oxide, HCNO, underwent addition of a water molecule, to form the hydroxyformaldoxime species (**iv**). The *in situ* generated Cu+ species preferentially coordinated to the *N*-donor atom of (**iv**) causing labilization of the C−O and N−O bonds (**v**). Thereafter, the HCN species (**vi**) was generated, releasing a molecule of hydrogen peroxide [38]. The generated HCN species then enters the organometallic cycle (Figure **2.3**, **C**) at the stage of ligand exchange. The representative 4−Iodoanisole (**12a**) oxidatively adds to the active Cu(I) complex, forming an aryl Cu(III) species (**D**). It undergoes ligand exchange with HCN to form (**E**), which on reductive elimination yielded 4-methoxybenzonitrile (**13a**) with simultaneous regeneration of $[Cu(phen)_2]^+$ complex.

2.3.5 *Computational Study*

Along with the experimental analysis, to look into the heart of the electronic structure at atomistic level, DFT calculations have been performed to gain an in-depth mechanistic insight for the *in situ* generation of HCN. A potential energy surface (PES) is constructed to investigate the detailed mechanism with energetics (Figure **2.4**). The potential energy surface was built by considering the ground state energies of initial reactants as zero. The absolute energies and relative energies are presented in Table **2.3**.

The formation of species (**i**) proceeded *via* a transition state, **TS1** (imaginary frequency = 1146i cm^{-1}) where, one of the C−H bonds of nitromethane interacted with K_2CO_3 and undergone an elongation from 1.09 Å to 1.35 Å to release HCO_3^{2-}. This step had an activation barrier of 11.27 kcal/mol and was spontaneous, with Gibbs free energy

change (ΔG) of -0.9 kcal/mol. **TS2** marked the elongation of the O−H bond of HCO_3^{2-} from 0.976 Å to 1.35 Å resulting in the formation of (**ii**), a new O−H bond with a bond distance of 1.12 Å. Only one imaginary frequency (680i cm^{-1}) was obtained with an activation barrier of 11.35 kcal/mol and ΔG value of 13.53 kcal/mol. Species (**ii**) then underwent dehydration to generate HCNO (**iii**). This step was a barrierless transition (barrier of activation is -0.5 kcal/mol, imaginary frequency = 278i cm^{-1}) which may be due to the presence of a good leaving group (H$_2$O) in the transition state (**TS3**). The resultant HCNO species (**iii**) was quite stable, as represented in the PES. The process was spontaneous with ΔG = −14.07 kcal/mol. The addition of a molecule of H$_2$O to HCNO species to form hydroxyformaldoxime (**iv**) passed through **TS4** (imaginary frequency of 105i cm^{-1}) with a very low barrier of 1.01 kcal/mol; the process was spontaneous with ΔG = −0.20 kcal/mol.
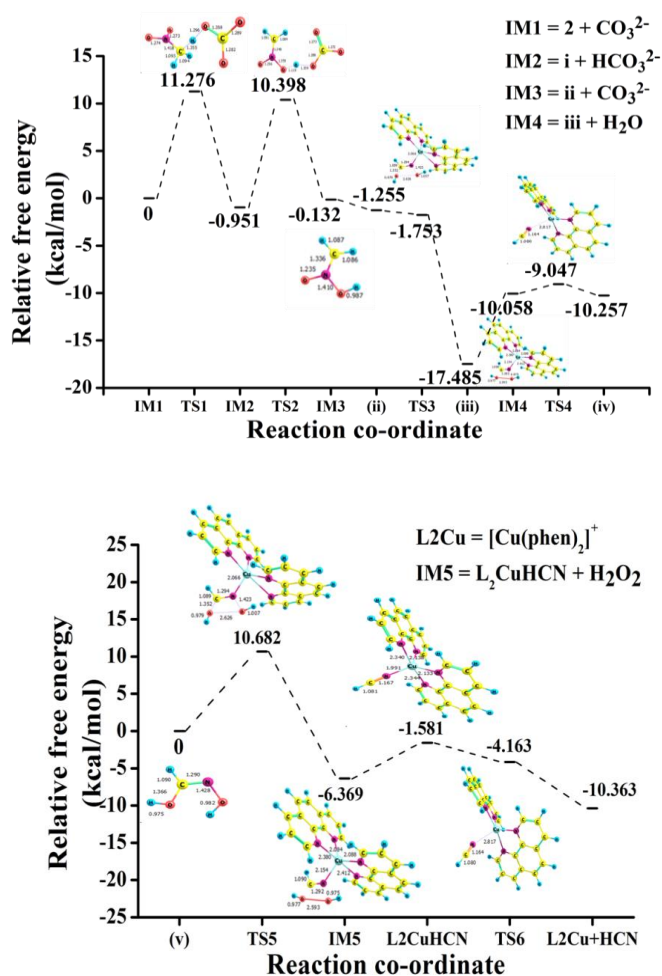

Figure **2.4** Potential energy surfaces depicting the generation of HCN from nitromethane at RPBE/DNP level of theory.

TD-DFT spectrum of $[Cu(phen)_2]^+$ confirmed the formation of Cu(I) complex with λ_{max} = 417 nm (Figure **2.5**) in correlation to the experimental absorption intensity (λ_{max}) at 420 nm.
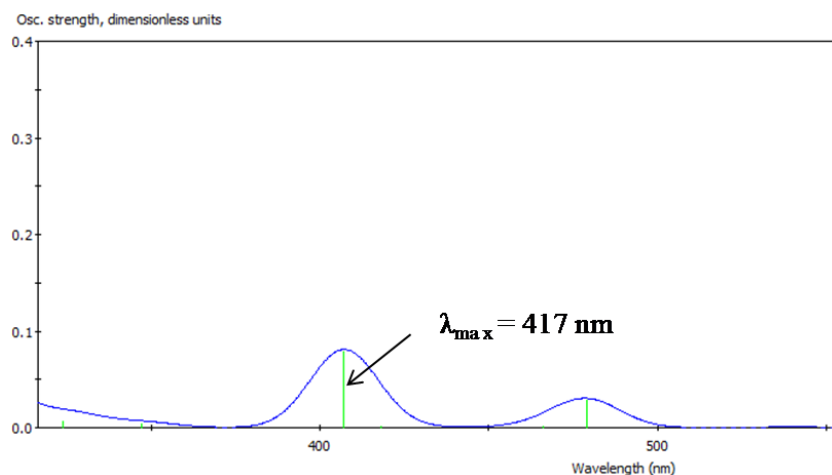

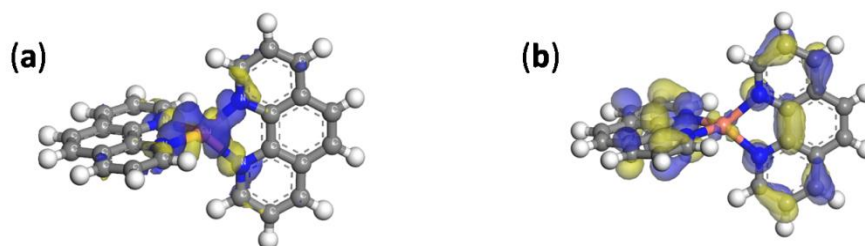Figure **2.5** TD-DFT spectrum of $[Cu(phen)_2]^+$ complex at RPBE/DNP level of theory

Figure **2.6** (**a**) Metal-centered HOMO of $[Cu(phen)_2]^+$; (**b**) Ligand-centered LUMO of $[Cu(phen)_2]^+$

The metal to ligand charge transfer (MLCT) is depicted by the metal-centered HOMO and the ligand-centered LUMO of $[Cu(phen)_2]^+$ complex (Figure **2.6**). $[Cu(phen)_2]^+$ complex interacted with species (**iv**) to form (**v**) (pre-reaction complex). In (**v**), the two Cu-N bonds of $[Cu(phen)_2]^+$ elongated from 2.08 Å to 2.30 Å and 2.44 Å respectively. Moreover, the bond distances of O-H groups from each other in (**iv**) changed from 2.65 Å to 2.13 Å in (**v**). Thus, transition (**TS5**) took place with an activation barrier of 10.68 kcal/mol, (imaginary frequency = 499i cm^{-1}) and Gibbs free energy change (ΔG) of -6.36 kcal/mol to form IM5. The formation of H_2O_2 in IM4 triggered the generation of HCN. This transition (**TS6**) was barrierless with Gibbs free energy change of ΔG = -8.7 kcal/mol. From the PES (Figure **2.4**), it was observed that the post reaction complex ($L_2Cu+HCN$) was a reasonably stable species. Only one imaginary frequency provides

testimony of the transition states connecting the reactants and products. Optimized geometries of all the species involved in the generation of HCN from nitromethane are shown in Figure **2.7**.

Table **2.3** Absolute energies and relative energies of the steps involved in the generation of HCN from nitromethane at RPBE/DNP level of theory. Values are in kcal/mol at 100 °C.

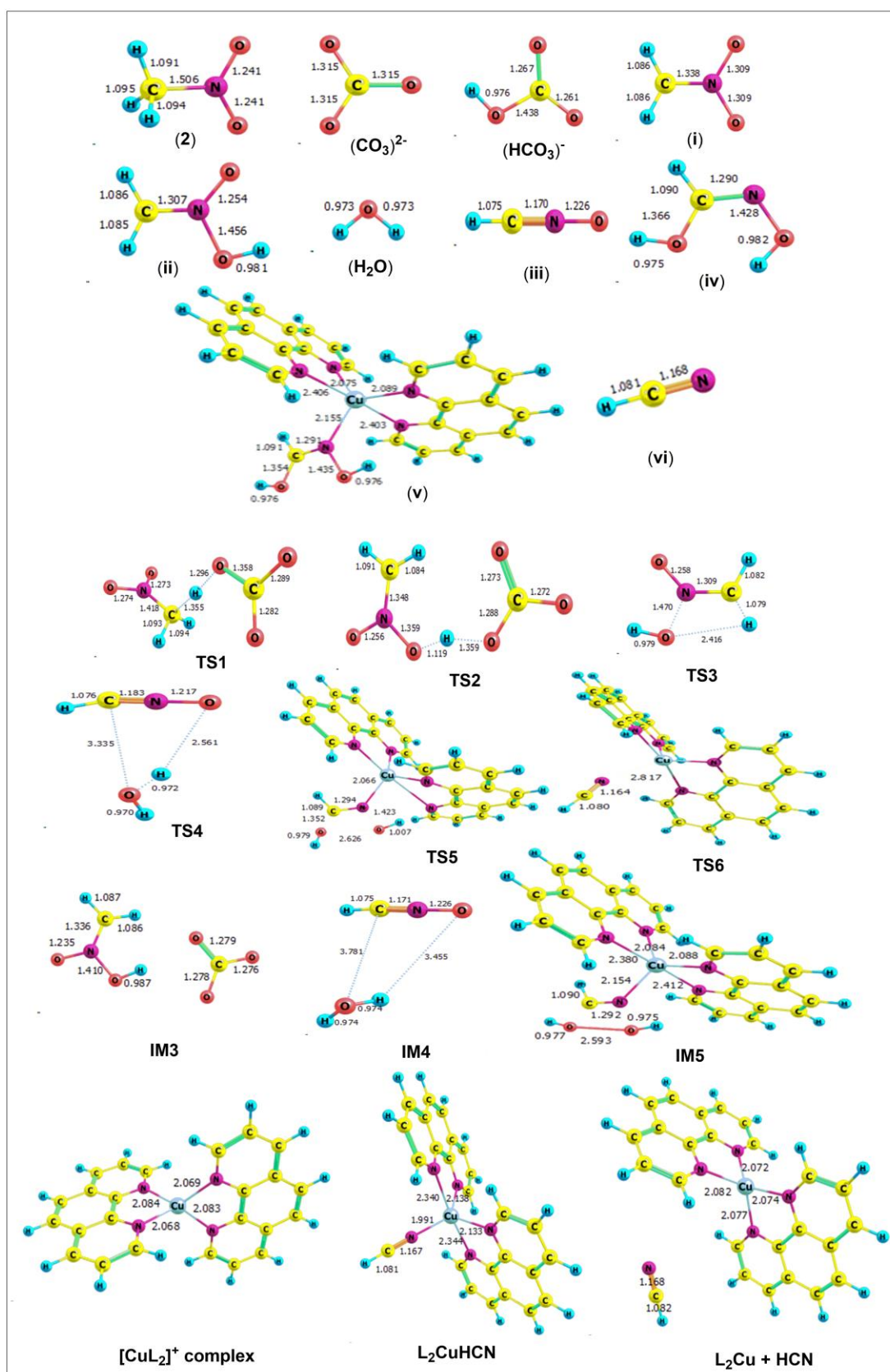|	Absolute Energies (Kcal/mol)	Relative Energies (Kcal/mol)
IM1	−3.686	0
TS1	7.59	11.276
IM2	−4.637	−0.951
TS2	6.712	10.398
IM3	8.894	−0.132
(ii)	7.771	−1.255
TS3	7.273	−1.753
(iii)	−6.294	−17.485
IM4	−1.032	−10.058
TS4	−0.021	−9.047
(iv)	−1.231	−10.257
(v)	178.131	0
TS5	188.813	10.682
IM5	171.762	−6.369
L_2CuHCN	174.156	−1.581
TS6	171.574	−4.163
$L_2Cu+HCN$	165.374	−10.363

Figure **2.7** Optimized geometries of all the species involved in the generation of HCN from nitromethane at RPBE/DNP level of theory (ball and stick model).

2.3.6 *Conclusion*

To summarize this chapter, we have developed a simple Cu^I catalyzed methodology for the generation of synthetically and pharmaceutically important aryl nitriles, with nitromethane as the cyanating source. Easily synthesizable $[Cu(phen)_2]^{2+}$ catalyst ensured homogeneity of the reaction medium, surpassing the risk of catalyst deactivation. Operational simplicity of the method overcame most drawbacks associated with usual cyanation processes. We have demonstrated the first detailed outlook on the unusual mechanism of generation of a CN^- species from nitromethane, with simultaneous *in situ* reduction of Cu^{II} to Cu^I. We believe that our study will lead to newer avenues on nitromethane and its extensive utilization in synthetic organic chemistry.

### *2.3.7 Experimental Section*

2.3.7.1 *General Information*

All the chemicals used for the reactions were procured commercially and used without further purification. The progress of the reaction was monitored through thin layer chromatography on Merck Kieselgel Silica gel 60 F_{254} plates using short wave UV light (λ=254 nm). The products were purified by column chromatography using Silica gel (60-120 mesh and 100-200 mesh). The identification of the purified products was carried out by NMR spectroscopy. The ^1H and ^{13}C NMR spectra were recorded on a 400 MHz JEOL NMR spectrometer (400 MHz for ^1H and 100 MHz for ^{13}C). Chemical shifts for both ^1H (δ_H) and ^{13}C (δ_C) NMR are assigned in parts per million (ppm) using TMS (0 ppm) as the internal reference and $CDCl_3$ and DMSO-d_6 as solvent ($CDCl_3$: δ_H = 7.25 ppm and δ_C = 77.1 ppm; DMSO-d_6: δ_H = 2.5 ppm, DMSO-d_6 absorbed water = 3.3 ppm and δ_C = 40.0 ppm). The multiplicities of the signals are assigned as: s = singlet, d = doublet, t = triplet, br = broad and m = multiplet. HRMS data were recorded in Q–TQF mass analyzer by electron spray ionization technique.

All the computation was performed as in Dmol^3 program package [39,40]. Generalized gradient approximation (GGA) using revised Perdew-Burke-Ernzerhof exchange-correlation functional has been used to optimize the electronic structures of the reactants, pre-reactive complexes (RCs), transition states (TSs) and products with

double numerical with polarization (DNP) basis set for our calculations [41]. DNP basis set used for our calculations was comparable to Gaussian 6-31G**, but DNP was more accurate than a Gaussian basis set of the same size [42,43]. For the vibrational frequency calculations, same level of theory was used. We obtained stable minima which corresponded to the real and positive values and the first order saddle points (transition states) were characterized by imaginary frequency. To improve computational performance, a global orbital cutoff of 4.5 Å was employed. Self-consistent field (SCF) procedures were done with tolerances of the energy, gradient and displacement convergences: 1.0×10^{-5} Ha, 2×10^{-3} Ha Å and 5×10^{-3} Å respectively. RPBE functional has been preferred for the calculations as it displayed better results with good accuracy comprehensive for improved adsorption energies of small molecules on transition metal complexes, which was the ultimate goal of this study. The effect of solvent continuum, in DMSO was incorporated using conductor-like screening model (COSMO) in $Dmol^3$ module. Temperature ranging from 25 K to 1000 K at an interval of 25 has been carried out. Analysis of 373 K in correlation to the experimental run to simulate the same environment has been performed.

2.3.7.2 *General experimental procedure for the synthesis of aryl nitriles (13a-k)*
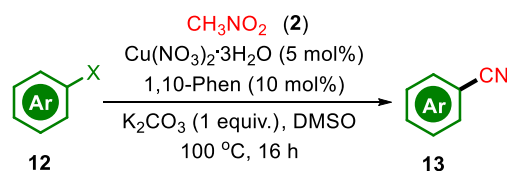
An oven-dried 50 mL round-bottomed flask, with a magnetic stirring bar, was charged with $Cu(NO_3)_2 \cdot 3H_2O$ (5 mol%, 0.05 mmol, 0.0123 g), 1,10–Phenanthroline monohydrate (10 mol%, 0.1 mmol, 0.0199 g), nitromethane, **2** (1.5 equiv., 1.5 mmol, 80 µL) aryl halide, **12** (1 mmol), K_2CO_3 (1 equiv., 0.138 g) in DMSO (4 mL). It was then fitted to a condenser and stirred at 100 °C under reflux conditions in an oil bath. After 16 h, the crude mixture was extracted with EtOAc and washed with crushed ice. The organic phase was dried over anhydrous Na_2SO_4 and concentrated under reduced pressure. The resulting reaction mixture was purified by column chromatography using hexane-EtOAc mixture as eluent to afford product **13**. Further, the products were checked for the presence of Cu, if any, by ICP-AES.

2.3.7.3 *Synthesis and Characterization of [Cu(phen)$_2$]$^{2+}$*

Cu(NO$_3$)$_2$·3H$_2$O (0.5 mmol, 0.1204 g), 1,10-Phenanthroline monohydrate (1 mmol, 0.2101 g) and K$_2$CO$_3$ (1 mmol, 0.1392 g) in DMSO (4 mL) were added to a 50 mL round-bottomed flask fitted to a condenser at 100 °C under reflux conditions in an oil bath for 5 hours. The resultant water-soluble blue-black precipitate was filtered, washed with methanol followed by diethyl ether and dried in a vaccum dessicator. It was then characterized by HRMS−ESI and confirmed to be [Cu(phen)$_2$]$^{2+}$.

HRMS−ESI calculated for [C$_{24}$H$_{16}$CuN$_4$]$^+$: 423.0671; found: 423.0687.

2.3.7.4 *Picrate paper test*

Picrate paper was prepared by dipping a filter paper in a 0.5% w/v solution of moist picric acid in 2.5% w/v NaHCO$_3$, allowing the paper to dry in air and then cutting to the required size. The picrate paper strip was then inserted into the reaction flask. The change in colour of the picrate paper strip from yellow to red indicated the evolution of CN$^-$ in the reaction medium.

2.3.8 *Characterization data for aryl nitrile derivatives (13a-k):*

4−Methoxybenzonitrile (**13a**)
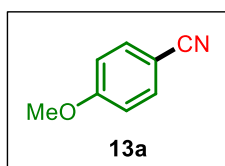
Synthesized as per the general experimental procedure (from X=I, 85%, 113 mg and X=Br, 68%, 90 mg); obtained as a colourless solid, ^{1}H NMR (400 MHz, CDCl$_3$): δ_H (ppm) 3.84 (s, 3H), 6.93 (d, J = 8 Hz, 2H), 7.56 (d, J = 8 Hz, 2H); ^{13}C NMR (100 MHz, CDCl$_3$): δ_C (ppm) 55.6, 104.0, 114.8, 119.3, 134.0, 162.9. Spectroscopic data was consistent with literature [44].
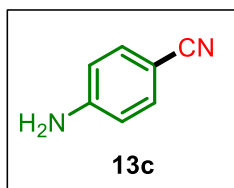
Benzonitrile (**13b**)
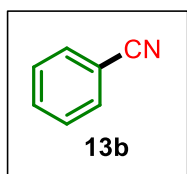
Synthesized as per the general experimental procedure (from X=I, 50%, 52 mg); obtained as a colourless oil, ^{1}H NMR (400 MHz, DMSO−d_6): δ_H (ppm) 7.54 (t, J = 8 Hz, 2H), 7.69 (t, J = 8 Hz, 1H), 7.80 (d, J = 8 Hz 2H); ^{13}C NMR (100 MHz, DMSO−d_6): δ_C (ppm) 111.8, 119.3, 130.0, 132.7, 133.8. Spectroscopic data was
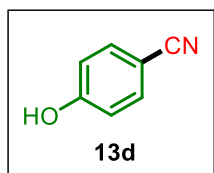
consistent with literature [44].
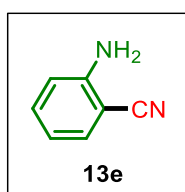
4−Aminobenzonitrile (**13c**)

Synthesized as per the general experimental procedure (from X=I, 72%, 85 mg and X=Br, 65%, 76 mg); obtained as a colourless solid, ^{1}H NMR (400 MHz, DMSO−d_6): δ_H (ppm) 6.08 (br s, 2H), 6.56 (d, J = 8 Hz, 2H), 7.34 (d, J = 8 Hz, 2H); ^{13}C NMR (100 MHz, DMSO−d_6): δ_C (ppm) 95.9, 113.9, 121.1, 133.9, 153.5. Spectroscopic data was consistent with literature [44].

4−Hydroxybenzonitrile (**13d**)

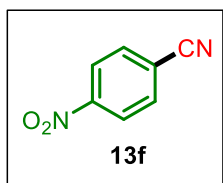Synthesized as per the general experimental procedure (from X=I, 80%, 95 mg); obtained as a colourless solid, ^{1}H NMR (400 MHz, DMSO−d_6): δ_H (ppm) 6.86 (d, J = 8 Hz, 2H), 7.59 (d, J = 8 Hz, 2H), 10.57 (s, 1H); ^{13}C NMR (100 MHz, DMSO−d_6): δ_C (ppm) 101.4, 116.9, 120.0, 134.7, 162.1. Spectroscopic data was consistent with literature [44].
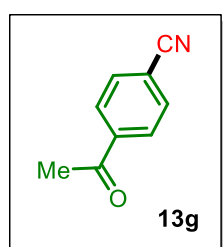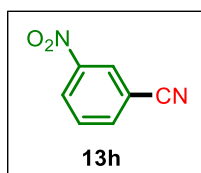
2−Aminobenzonitrile (**13e**)

Synthesized as per the general experimental procedure (from X=I, 52%, 61 mg and 2-Nitroiodobenzene, 73%, 86 mg); obtained as a light yellow solid, ^{1}H NMR (400 MHz, DMSO−d_6): δ_H (ppm) 5.97 (s, 2H), 6.54 (t, J = 8 Hz, 1H), 6.73 (d, J = 8 Hz, 1H), 7.25 (t, J = 8 Hz, 1H), 7.32 (d, J = 8 Hz, 1H); ^{13}C NMR (100 MHz, DMSO−d_6): δ_C (ppm) 93.8, 115.6, 116.4, 118.6, 132.9, 134.4, 152.1. HRMS−ESI calculated for [$C_7H_6N_2$]$^+$: 118.0531; found: 118.0860.
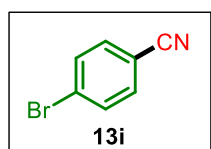
4-Nitrobenzonitrile (**13f**)

Synthesized as per the general experimental procedure (from X=I, 78%, 115 mg and X=Br, 72%, 107 mg); obtained as a off white solid, ^{1}H NMR (400 MHz, CDCl$_3$): δ_H (ppm) 7.88 (d, J = 8.8 Hz, 2H), 8.34 (d, J = 8 Hz, 2H); ^{13}C NMR (100 MHz, CDCl$_3$): δ_C (ppm) 116.8, 118.4, 124.3, 133.5. Spectroscopic data was consistent with literature [45].

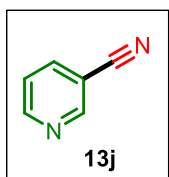## 4−Acetylbenzonitrile (**13g**)

Synthesized as per the general experimental procedure (from X=I, 70%, 102 mg and X=Br, 54%, 78 mg); obtained as a colourless solid, ^{1}H NMR (400 MHz, CDCl$_3$): δ_H (ppm) 2.63 (s, 3H), 7.76 (d, J = 8 Hz, 2H), 8.03 (d, J = 8 Hz, 2H); ^{13}C NMR (100 MHz, CDCl$_3$): δ_C (ppm) 26.8, 116.5, 118.0, 128.7, 132.6, 139.9, 196.6. Spectroscopic data was consistent with literature [45].

3−Nitrobenzonitrile (**13h**)

Synthesized as per the general experimental procedure (from X=I, 61%, 90 mg); obtained as a off white solid, ^{1}H NMR (400 MHz, DMSO−d_6): δ_H (ppm) 7.84 (t, J = 8 Hz, 1H), 8.27 (d, J = 8 Hz, 1H), 8.49 (d, J = 8 Hz, 1H), 8.70 (s, 1H); ^{13}C NMR (100 MHz, DMSO−d_6): δ_C (ppm) 113.3, 117.5, 127.9, 128.5, 131.7, 139.0, 148.4. Spectroscopic data was consistent with literature [46].

4−Bromobenzonitrile (**13i**)

Synthesized as per the general experimental procedure (from X=I, 65%, 118 mg); obtained as a colourless solid, ^{1}H NMR (400 MHz, CDCl$_3$): δ_H (ppm) 7.51 (d, J = 8 Hz, 2H), 7.61 (d, J = 8 Hz, 2H); ^{13}C NMR (100 MHz, CDCl$_3$): δ_C (ppm) 111.3, 118.2, 128.1, 132.7, 133.5. Spectroscopic data was consistent with literature [45].

Pyridine−3−carbonitrile (**13j**)

Synthesized as per the general experimental procedure (from X=Br, 63%, 65 mg); obtained as a light yellow oil, ^{1}H NMR (400 MHz, DMSO−d_6): δ_H (ppm) 7.58-7.61 (m, 1H), 8.29 (d, J = 8 Hz, 1H), 8.83 (d, J = 8 Hz, 1H), 8.99 (s, 1H); ^{13}C NMR (100 MHz, DMSO−d_6): δ_C (ppm) 109.7, 117.6, 124.6, 140.6, 153.0, 153.8. Spectroscopic data was consistent with literature [44].

2−Phenylacetonitrile (**13k**)
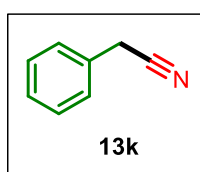
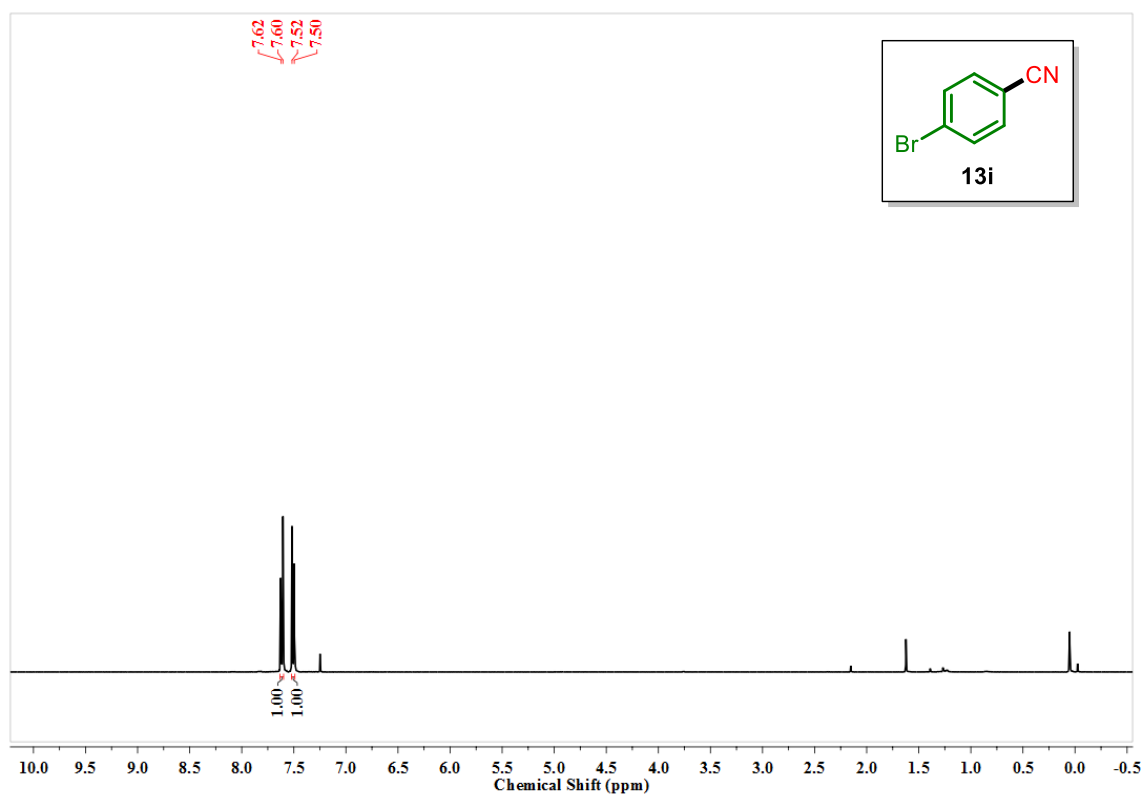Synthesized as per the general experimental procedure (from X=Br, 75%, 88 mg); obtained as a colourless liquid, ^{1}H NMR (400 MHz, DMSO−d_6): δ_H (ppm) 3.99 (s, 2H), 7.27-7.32 (m, 3H), 7.36 (t, J = 8 Hz, 2H); ^{13}C NMR (100 MHz, DMSO−d_6): δ_C (ppm) 22.9, 119.7, 128.1, 128.5, 129.4, 131.8. Spectroscopic data was consistent with literature [47].

2.3.9 *Representative ¹H and ¹³C NMR spectra of aryl nitrile derivatives:*

Figure **2.8** ¹H NMR spectrum of **13i** in CDCl$_3$ (400 MHz, 298 K)
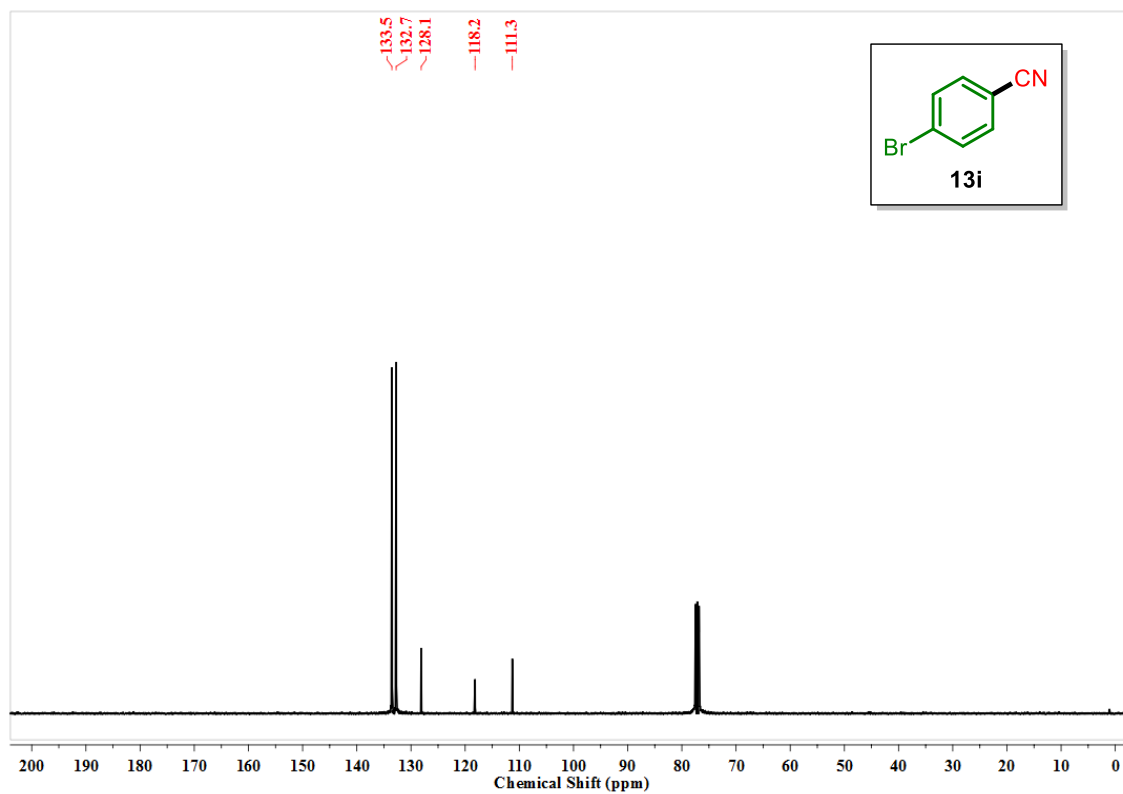
Figure **2.9** ¹³C NMR spectrum of **13i** in CDCl$_3$ (100 MHz, 298 K)
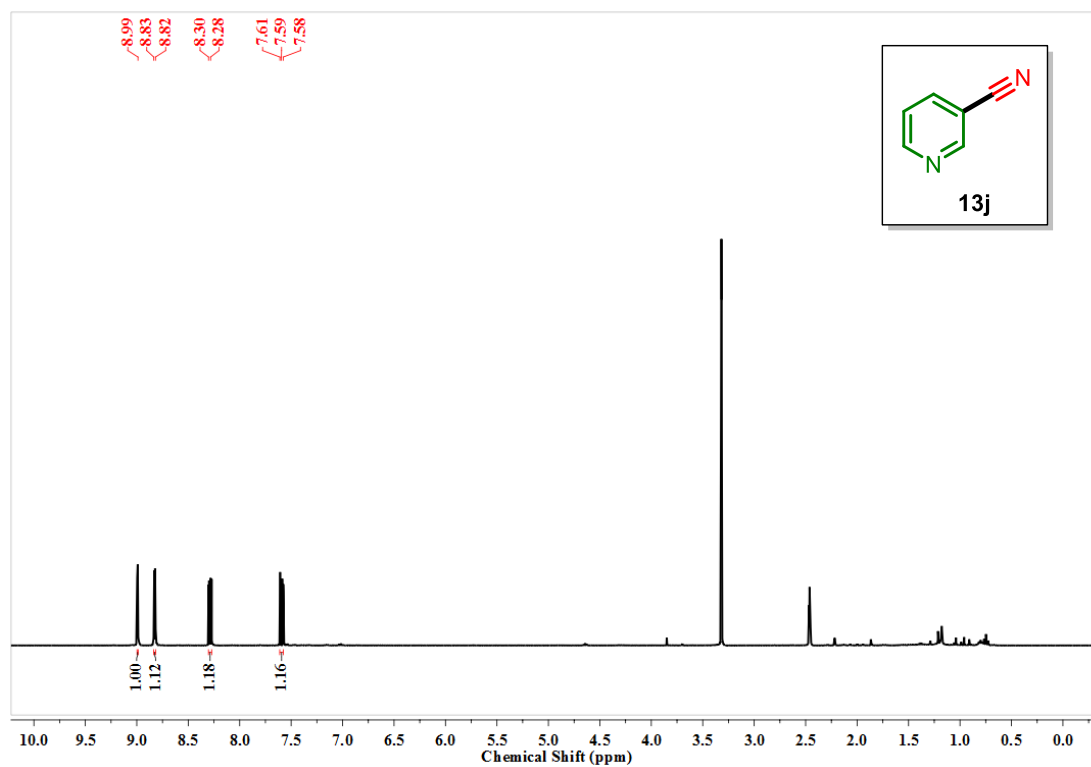
Figure **2.10** ^{1}H NMR spectrum of **13j** in DMSO−d_6 (400 MHz, 298 K)
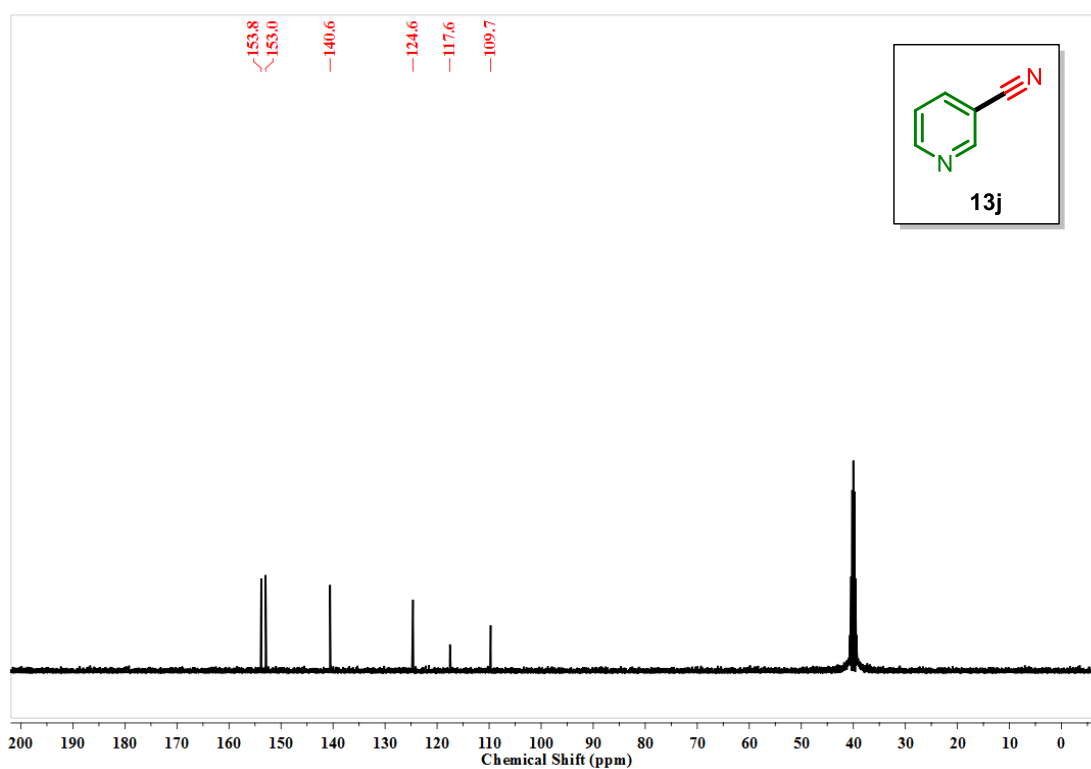
Figure **2.11** ^{13}C NMR spectrum of **13j** in DMSO−d_6 (100 MHz, 298 K)

2.4 *Bibliography*

[1] Pimparkar, S., Koodan, A., Maiti, S., Ahmed, N. S., Mostafa, M. M. M., and Maiti, D. C–CN bond formation: An overview of diverse strategies. *Chemical Communications*, 57(18):2210-2232, 2021.

[2] Peng, J., Zhao, J., Hu, Z., Liang, D., Huang, J., and Zhu, Q. Palladium–catalyzed C (sp^2)–H cyanation using tertiary amine derived isocyanide as a cyano source. *Organic Letters*, 14(18):4966-4969, 2012.

[3] Higashimae, S., Kurata, D., Kawaguchi, S. I., Kodama, S., Sonoda, M., Nomoto, A., and Ogawa, A. Palladium-catalyzed cyanothiolation of internal alkynes using organic disulfides and *tert*-butyl isocyanide. *The Journal of Organic Chemistry*, 83(9):5267-5273, 2018.

[4] Shirsath, S. R., Shinde, G. H., Shaikh, A. C., and Muthukrishnan, M. Accessing α–arylated nitriles *via* BF$_3$·OEt$_2$ catalyzed cyanation of *para*-Quinone Methides using *tert*-butyl isocyanide as a cyanide source. *The Journal of Organic Chemistry*, 83(19):12305-12314, 2018.

[5] Zhang, L., Lu, P., and Wang, Y. Cu(NO$_3$)$_2$·3H$_2$O–mediated cyanation of aryl iodides and bromides using DMF as a single surrogate of cyanide. *Chemical Communications*, 51(14):2840-2843, 2015.

[6] Zhang, L., Lu, P., and Wang, Y. Copper-mediated cyanation of indoles and electron-rich arenes using DMF as a single surrogate. *Organic & Biomolecular Chemistry*, 13(30):8322-8329, 2015.

[7] Wang, Z., and Wu, X. F. Applications of DMF as a Reagent in Organic Synthesis. In Ding, K., Wu, X. F., Han, B., Liu, Z., editors, *The Chemical Transformations of C1 Compounds*, *Volume 2,* pages 1439-1474, Wiley-VCH, 2022.

[8] Cai, X. H., and Guo, H. *N*,*N*–dimethylformamide (DMF): An Inexpensive and Attractive Reactant. *Current Organic Chemistry*, 25(17):1977-2004, 2021.

[9] Niknam, E., Panahi, F., and Khalafi-Nezhad, A. Palladium-Catalyzed Cyanation of Aryl Halides Using Formamide and Cyanuric Chloride as a New "CN" Source. *European Journal of Organic Chemistry*, 2020(18):2699-2707, 2020.

[10]   Yang, L., Liu, Y. T., Park, Y., Park, S. W., and Chang, S. Ni–mediated generation of "CN" unit from formamide and its catalysis in the cyanation reactions. *ACS Catalysis*, 9(4):3360-3365, 2019.

[11]   Deng, L. F., Cheng, J., Chen, J. J., and Yang, L. Ni-Catalyzed Cyanation of Allylic Alcohols with Formamide as the Cyano Source. *European Journal of Organic Chemistry*, 2022(25):e202200339, 2022.

[12]   Zhao, L., Dong, Y., Xia, Q., Bai, J., and Li, Y. Zn–catalyzed cyanation of aryl iodides. *The Journal of Organic Chemistry*, 85(10):6471-6477, 2020.

[13]   Shu, X., Jiang, Y. Y., Kang, L., and Yang, L. Ni-Catalyzed hydrocyanation of alkenes with formamide as the cyano source. *Green Chemistry*, 22(9):2734-2738, 2020.

[14]   Zhang, J., Luo, C. P., and Yang, L. Nickel/Cobalt–Catalyzed Reductive Hydrocyanation of Alkynes with Formamide as the Cyano Source, Dehydrant, Reductant, and Solvent. *Advanced Synthesis & Catalysis*, 363(1):283-288, 2021.

[15]   Murugesan, K., Senthamarai, T., Sohail, M., Sharif, M., Kalevaru, N. V., and Jagadeesh, R. V. Stable and Reusable Nanoscale Fe_2O_3–Catalyzed Aerobic Oxidation Process for the Selective Synthesis of Nitriles and Primary Amides. *Green Chemistry*, 20(1):266-273, 2018.

[16]   [a] Maestri, G., Caneque, T., Della Ca', N., Derat, E., Catellani, M., Chiusoli, G. P., and Malacria, M. Pd Catalysis in Cyanide-Free Synthesis of Nitriles from Haloarenes *via* Isoxazolines. *Organic Letters*, 18(23):6108-6111, 2016; [b] Jia, X., Yang, D., Zhang, S., and Cheng, J. Chelation-Assisted Palladium-Catalyzed Direct Cyanation of 2-Arylpyridine C–H Bonds. *Organic Letters*, 11(20):4716-4719, 2009; [c] Sundermeier, M., Zapf, A., Mutyala, S., Baumann, W., Sans, J., Weiss, S., and Beller, M. Progress in the Palladium-Catalyzed Cyanation of Aryl Chlorides. *Chemistry–A European Journal*, 9(8):1828-1836, 2003.

[17]   Zhang, X., Xia, A., Chen, H., and Liu, Y. General and Mild Nickel-Catalyzed Cyanation of Aryl/Heteroaryl Chlorides with $Zn(CN)_2$: Key roles of DMAP. *Organic Letters*, 19(8):2118-2121, 2017.

[18]   [a] Li, J., and Ackermann, L. Cobalt-catalyzed C-H Cyanation of Arenes and Heteroarenes. *Angewandte Chemie International Edition*, 54(12):3635-3638, 2015; [b] Yu, D. G., Gensch, T., de Azambuja, F., Vasquez-Cespedes, S., and Glorius, F. Co(III)-Catalyzed C–H Activation/Formal S_N-Type Reactions: Selective

and Efficient Cyanation, Halogenation and Allylation. *Journal of the American Chemical Society*, 136(51):17722-17725, 2014.

[19] Nagase, Y., Sugiyama, T., Nomiyama, S., Yonekura, K., and Tsuchimoto, T. Zinc-Catalyzed Direct Cyanation of Indoles and Pyrroles: Nitromethane as a Source of a Cyano Group. *Advanced Synthesis & Catalysis*, 356(2-3):347-352, 2014.

[20] Chaitanya, M., Yadagiri, D. and Anbarasan, P. Rhodium Catalyzed Cyanation of Chelation Assisted C–H Bonds. *Organic Letters*, 15(19):4960-4963, 2013.

[21] Murahashi, S. I., Komiya, N., Terai, H., and Nakae, T. Aerobic Ruthenium-Catalyzed Oxidative Cyanation of Tertiary Amines with Sodium Cyanide. *Journal of the American Chemical Society*, 125(50):15312-15313, 2003.

[22] Ping, Y., Ding, Q., and Peng, Y. Advances in C–CN bond formation *via* C–H bond activation. *ACS Catalysis*, 6(9):5989-6005, 2016.

[23] Wen, Q., Jin, J., Zhang, L., Luo, Y., Lu, P., and Wang, Y. Copper-Mediated Cyanation Reactions. *Tetrahedron Letters*, 55(7):1271-1280, 2014.

[24] [a] Schareina, T., Zapf, A., Mägerlein, W., Müller, N., and Beller, M. A State-of-the-Art Cyanation of Aryl Bromides: A Novel and Versatile Copper Catalyst System Inspired by Nature. *Chemistry–A European Journal*, 13(21):6249-6254, 2007; [b] Anbarasan, P., Neumann, H., and Beller, M. A Novel and Convenient Synthesis of Benzonitriles: Electrophilic Cyanation of Aryl and Heteroaryl Bromides. *Chemistry–A European Journal*, 17(15):4217-4222, 2011.

[25] Chen, X., Hao, X. S., Goodhue, C. E., and Yu, J. Q. Cu(II)-Catalyzed Functionalizations of Aryl C–H bonds using O_2 as an oxidant. *Journal of the American Chemical Society*, 128(21):6790-6791, 2006.

[26] Motokura, K., Matsunaga, K., Miyaji, A., Yamaguchi, S., and Baba, T. A. Method for the Cyanation of Alkenes using Nitromethane as a Source of Cyano Group Mediated by Proton-Exchanged Montmorillonite. *Tetrahedron Letters*, 55(51):7034-7038, 2014.

[27] Wang, Z. H., Ji, X. M., Hu, M. L., and Tang, R. Y. Nitromethane as a Cyanating Reagent for the Synthesis of Thiocyanates. *Tetrahedron Letters*, 56(36):5067-5070, 2015.

[28] Ogiwara, Y., Morishita, H., Sasaki, M., Imai, H., and Sakai, N. Copper-Catalyzed Cyanation of Aryl Iodides Using Nitromethane. *Chemistry Letters*, 46(12):1736-1739, 2017.

[29] Suzuka, T., Niimi, R., and Uozumi, Y. Cyanide-Free Cyanation of Aryl Iodides with Nitromethane by Using an Amphiphilic Polymer-Supported Palladium Catalyst. *Synlett*, 33(01):40-44, 2022.

[30] Øpstad, C. L., Melø, T. B., Sliwka, H. R., and Partali, V. Formation of DMSO and DMF Radicals with Minute Amounts of Base. *Tetrahedron*, 65(36):7616-7619, 2009.

[31] [a] Sandroni, M., Pellegrin, Y., and Odobel, F. Heteroleptic *Bis*-diimine Copper(I) Complexes for Applications in Solar Energy Conversion. *Comptes Rendus Chimie*, 19(1-2):79-93, 2016; [b] Cunningham, C. T., Moore, J. J., Cunningham, K. L., Fanwick, P. E., and McMillin, D. R. Structural and Photo-physical Studies of Cu $(NN)^{2+}$ Systems in the Solid State. Emission at Last from Complexes with Simple 1,10-Phenanthroline Ligands. *Inorganic Chemistry*, 39(16):3638-3644, 2000; [c] Armaroli, N. Photoactive Mono-and Polynuclear Cu(I)–Phenanthrolines. A Viable Alternative to Ru(II)–Polypyridines. *Chemical Society Reviews*, 30(2):113-124, 2001.

[32] Yuan, B., Zhu, Y., and Xu, K. The Study on 1,10-Phenanthroline-Copper Complex by CV-Thin Layer Spectroelectrochemistry. *International Journal of Electrochemical Science*, 10:4138-4145, 2015.

[33] Kumar, R., and Mathur, P. Aerobic Oxidation of 1,10-Phenanthroline to Phendione Catalyzed by Copper(II) Complexes of a Benzimidazolyl Schiff Base. *RSC Advances*, 4(63):33190-33193, 2014.

[34] [a] Zhang, G., Ren, X., Chen, J., Hu, M., and Cheng, J. Copper-Mediated Cyanation of Aryl Halide with the Combined Cyanide Source. *Organic Letters*, 13(19):5004-5007, 2011; [b] Kim, J., Choi, J., Shin, K., and Chang, S. Copper-Mediated Sequential Cyanation of Aryl C–B and Arene C–H Bonds Using Ammonium Iodide and DMF. *Journal of the American Chemical Society*, 134(5):2528-2531, 2012.

[35] [a] Hsu, D. S. Y., and Lin, M. C. Laser Probing and Kinetic Modeling of NO and CO Production in Shock-Wave Decomposition of Nitromethane Under Highly Diluted Conditions. *Journal of Energetic Materials*, 3(2):95-127, 1985; [b] Homayoon, Z.,

Bowman, J. M., Dey, A., Abeysekera, C., Fernando, R., and Suits, A. G. Experimental and Theoretical Studies of Roaming Dynamics in the Unimolecular Dissociation of CH_3NO_2 to CH_3O+NO. *Zeitschrift für Physikalische Chemie*, 227(11):1267-1280, 2013.

[36] [a] Melius, C. F. Thermochemistry and Reaction Mechanisms of Nitromethane Ignition. *Le Journal de Physique IV*, 5(C4):C4-535-C4-548, 1995; [b] Kaiser, R. I., and Maksyutenko, P. A Mechanistical Study on Non-Equilibrium Reaction Pathways in Solid Nitromethane (CH_3NO_2) and D_3–nitromethane (CD_3NO_2) upon Interaction with Ionizing Radiation. *Chemical Physics Letters*, 631:59-65, 2015.

[37] [a] Itoh, S., Kishikawa, N., Suzuki, T., and Takagi, H. D. Syntheses, Structural Analyses and Redox Kinetics of Four-Coordinate $[CuL_2]^{2+}$ and Five-Coordinate $[CuL_2(solvent)]^{2+}$ Complexes (L= 6,6'-Dimethyl-2,2'-bipyridine or 2,9-Dimethyl-1,10-phenanthroline): Completely Gated Reduction Reaction of $[Cu(dmp)_2]^{2+}$ in Nitromethane. *Dalton Transactions*, 6:1066-1078, 2005; [b] Lim, M. D., Capps, K. B., Karpishin, T. B., and Ford, P. C. Further Evidence Supporting an Inner Sphere Mechanism in the NO Reduction of the Copper(II) Complex $Cu(dmp)_2^{2+}$ (dmp = 2,9-Dimethyl-1,10-phenanthroline). *Nitric Oxide*, 12(4):244-251, 2005; [c] Tran, D., Skelton, B. W., White, A. H., Laverman, L. E., and Ford, P. C. Investigation of the Nitric Oxide Reduction of the *Bis*(2,9-dimethyl-1,10-phenanthroline) Complex of Copper(II) and the Structure of $[Cu(dmp)_2(H_2O)](CF_3SO_3)_2$. *Inorganic Chemistry*, 37(10):2505-2511, 1998; [d] Tran, D., and Ford, P. C. Nitric oxide Reduction of the Copper(II) Complex $Cu(dmp)_2^{2+}$ (dmp= 2,9-Dimethyl-1,10-phenanthroline). *Inorganic Chemistry*, 35(9):2411-2412, 1996.

[38] [a] Pantazis, D. A., Tsipis, A. C., and Tsipis, C. A. Ab Initio Quantum Chemical Study of the Coordination Preferences and Catalytic Role of Cu^+ ions in the Dehydration Reactions of Hydroxyformaldoxime Conformers and the Oxidation of HCN to Hydroxyformaldoxime by Hydrogen Peroxide. *The Journal of Physical Chemistry A*, 106(7):1425-1440, 2002; [b] Hu, W. F., He, T. J., Chen, D. M., and Liu, F. C. Theoretical study of the CH_3NO_2 Unimolecular Decomposition Potential Energy Surface. *The Journal of Physical Chemistry A*, 106(32):7294-7303, 2002.

[39] Delley, B. An All-Electron Numerical Method for Solving The Local Density Functional for Polyatomic Molecules. *The Journal of Chemical Physics*, 92(1):508-517, 1990.

[40] Hammer, B. H. L. B., Hansen, L. B., and Nørskov, J. K. Improved Adsorption Energetics Within Density-Functional Theory Using Revised Perdew-Burke-Ernzerhof Functionals. *Physical Review B*, 59(11):7413, 1999.

[41] Delley, B. From Molecules to Solids with the DMol^3 Approach. *The Journal of Chemical Physics*, 113(18):7756-7764, 2000.

[42] Benedek, N. A., Snook, I. K., Latham, K., and Yarovsky, I. Application of Numerical Basis Sets to Hydrogen Bonded Systems: A Density Functional Theory Study. *The Journal of Chemical Physics*, 122(14):144102, 2005.

[43] Inada, Y., and Orita, H. Efficiency of Numerical Basis Sets for Predicting the Binding Energies of Hydrogen Bonded Complexes: Evidence of Small Basis Set Superposition Error Compared to Gaussian Basis Sets. *Journal of Computational Chemistry*, 29(2):225-232, 2008.

[44] Zhang, S., Neumann, H., and Beller, M. Pd-Catalyzed Cyanation of (Hetero) Aryl Halides by Using Biphosphine Ligands. *Chemistry–A European Journal*, 24(1):67-70, 2018.

[45] Zhang, G., Ren, X., Chen, J., Hu, M., and Cheng, J. Copper-Mediated Cyanation of Aryl Halide with the Combined Cyanide Source. *Organic Letters*, 13(19):5004-5007, 2011.

[46] Wu, Q., Luo, Y., Lei, A., and You, J. Aerobic Copper-Promoted Radical-Type Cleavage of Coordinated Cyanide Anion: Nitrogen Transfer to Aldehydes to Form Nitriles. *Journal of the American Chemical Society*, 138(9):2885-2888, 2016.

[47] Xia, A., Xie, X., Chen, H., Zhao, J., Zhang, C., and Liu, Y. Nickel-Catalyzed Cyanation of Unactivated Alkyl Chlorides or Bromides with $Zn(CN)_2$. *Organic Letters*, 20(23):7735-7739, 2018.